Organic & Biomolecular Chemistry

PAPER

Cite this: *Org. Biomol. Chem.*, 2016, **14**, 7707

Improved thrombin binding aptamer analogues containing inversion of polarity sites: structural effects of extra-residues at the ends†

A. Virgilio,[a] T. Amato,[a] L. Petraccone,[b] R. Filosa,[c] M. Varra,[a] L. Mayol,[a] V. Esposito*[a] and A. Galeone*[a]

Received 29th April 2016,
Accepted 19th July 2016

DOI: 10.1039/c6ob00931j

www.rsc.org/obc

In this paper, we report the investigations, based on NMR, molecular modelling, CD measurements and electrophoresis, of thrombin binding aptamer (TBA) analogues containing an extra-residue at the 3′-end or at both the ends of the original TBA sequence, linked through 3′–3′ or 5′–5′ phosphodiester bonds. The data indicate that most of the modified aptamers investigated adopt chair-like G-quadruplex structures very similar to that of the TBA and that stacking interactions occur between the 3′–3′ or 5′–5′ extra residues and the deoxyguanosines of the upper G-tetrad. A comparison of the thermodynamic data of TBA-A and TBA-T containing a 3′–3′ extra residue and their canonical versions clearly indicates that the 3′–3′ phosphodiester bond is fundamental in endowing the modified aptamers with remarkably higher thermal stabilities than the original TBA.

Introduction

Aptamers are usually DNA or RNA ligands endowed with high affinity and specificity toward their targets. Thanks to these properties, aptamers can find applications in both diagnostics and therapeutics, and represent a powerful tool in many research fields.[1] Not surprisingly, several interesting aptamers adopt G-quadruplex structures,[2] probably due to the high thermal stability characterizing this non-canonical nucleic acid conformation. Among these, the anticoagulant thrombin binding aptamer (TBA) shows peculiar structural features since it adopts a "chair-like" G-quadruplex conformation characterized by only two overlapping G-tetrads and three lateral loops (Fig. 1).[3] Although the TBA is one of the first aptamers to be discovered, it still arouses therapeutic interest and is the subject of several investigations, particularly taking into account that it is also endowed with antiproliferative properties.[4] This aptamer has been subjected to several chemical modifications concerning both the bases and the sugar-phosphate backbone, mostly aimed at (i) enhancing its affinity to thrombin; (ii) making it resistant in biological environments; (iii) improving its thermal stability under physiological conditions; (iv) supporting the studies on the aptamer–target interaction and, recently, (v) switching its activity from anticoagulant to antiproliferative.[5] A convincing number of studies have indicated that the loops are the parts of the TBA mainly involved in the interaction with thrombin. Therefore, most of the modifications aimed at increasing the affinity to the target and, then, the anticoagulant activity, have involved residues in loops. For example, TBA analogues have been investigated in which thymidine derivatives have replaced natural thymidines in the loops. Among these are the locked nucleic acid residues (LNA-T),[6] unlocked nucleic acid residues (UNA-U)[7] and other types of acyclic thymidines,[8] L-residues,[9] D- and L-isothymidines,[10] 5-hydroxymethyl-[11] and 5-fluoro-2′-deoxyuridines.[12] On the other hand, specific residues in the loops also contribute to the thermal stability, which in turn, is ultimately associated to the biological activity, taking into account the low melting temperature shown by the TBA under physiological conditions in which a prevalence of sodium ions occurs. Generally, enhanced stability or biological activity (or both, in specific cases) can be obtained by modifying the residues T3, T7 and T12.[7,8] Conversely, only in one case,[12] modifications concerning residues T4, T13 have resulted in improved properties of the TBA, while most of the alterations involving these residues and, sometimes T9, have proven to be detrimental for both stability and anticoagulant activity.[7a,8a,10] A minor amount of research studies have been devoted to improving

[a]*Department of Pharmacy, University of Naples Federico II, via D. Montesano, 49, 80131 Naples, Italy. E-mail: galeone@unina.it, verespos@unina.it; Tel: +39 081678542, +39 081678746*
[b]*Department of Chemical Sciences, University of Naples Federico II, via Cintia, I-80126 Naples, Italy*
[c]*Department of Experimental Medicine, Second University of Naples, via Costantinopoli 16, 80138 Naples, Italy*
†Electronic supplementary information (ESI) available. See DOI: 10.1039/c6ob00931j

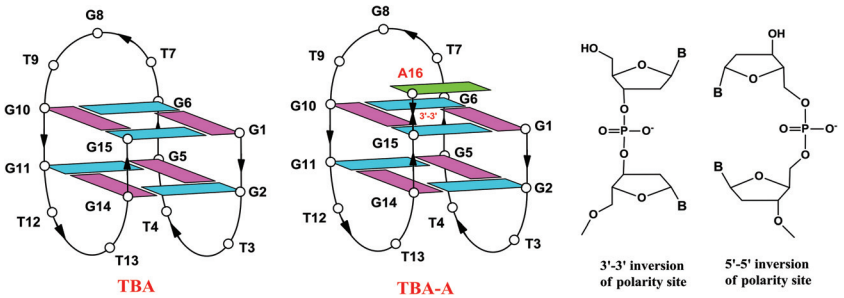

Fig. 1 Schematic representation of the G-quadruplex structures of TBA and TBA-A. Deoxyguanosines in *syn* and *anti* glycosidic conformations are in purple and light blue, respectively. The extra deoxyadenosine is in green. The chemical structures of the 3′–3′ and 5′–5′ inversion of polarity sites are reported on the right.

the resistance to nucleases. For example, modified TBAs containing 2′-deoxy-2′-fluoroarabinonucleotide residues,[13] L-residues,[9] thiophosphoryl[14] or triazole internucleotide bonds[15] have been proposed, although no noteworthy enhancements of the properties compared to the TBA have been reported in these cases. Recently, we have proposed a simple modification that consists of adding an extra-residue at the 3′-end or at both the ends of the TBA sequence, linked through 3′–3′ or 5′–5′ phosphodiester bonds (Table 1).[16] An advantage of this straightforward modification is that it does not affect the TT loops being mostly responsible for the interaction with the target protein. In fact, apart from endowing all modified aptamers with a remarkable resistance in biological environments, this approach has also provided some TBA derivatives with outstanding higher thermal stabilities and improved affinities to thrombin, in comparison with their natural counterpart.

With an aim to obtain more insights into the effects of this modification on the G-quadruplex structures and their relationship with the thermal stability, in this paper, we report a structural and physical–chemical analysis of the most interesting TBA derivatives based on NMR, polyacrylamide gel electrophoresis (PAGE), CD thermal denaturation experiments and molecular modelling. Among the TBA derivatives showing suitable NMR spectral features and a major conformation, those characterized by thermal stabilities and/or thrombin affinities similar to or higher than the natural TBA have been studied.

Table 1 Sequence and residue numbering of the oligodeoxynucleotides investigated. Extra residues have been labelled as N_0 (5′–5′ inversion) and N_{16} (3′–3′ inversion)

Name	Sequence
TBA	5′-$G_1G_2T_3T_4G_5G_6T_7G_8T_9G_{10}G_{11}T_{12}T_{13}G_{14}G_{15}$-3′
TBA-A	5′-$G_1G_2T_3T_4G_5G_6T_7G_8T_9G_{10}G_{11}T_{12}T_{13}G_{14}G_{15}$-3′-3′-$A_{16}$
TBA-T	5′-$G_1G_2T_3T_4G_5G_6T_7G_8T_9G_{10}G_{11}T_{12}T_{13}G_{14}G_{15}$-3′-3′-$T_{16}$
T-TBA-A	T_0-5′-5′-$G_1G_2T_3T_4G_5G_6T_7G_8T_9G_{10}G_{11}T_{12}T_{13}G_{14}G_{15}$-3′-3′-$A_{16}$
A-TBA-T	A_0-5′-5′-$G_1G_2T_3T_4G_5G_6T_7G_8T_9G_{10}G_{11}T_{12}T_{13}G_{14}G_{15}$-3′-3′-$T_{16}$
TBA-G	5′-$G_1G_2T_3T_4G_5G_6T_7G_8T_9G_{10}G_{11}T_{12}T_{13}G_{14}G_{15}$-3′-3′-$G_{16}$
TBA-C	5′-$G_1G_2T_3T_4G_5G_6T_7G_8T_9G_{10}G_{11}T_{12}T_{13}G_{14}G_{15}$-3′-3′-$C_{16}$
C-TBA-G	C_0-5′-5′-$G_1G_2T_3T_4G_5G_6T_7G_8T_9G_{10}G_{11}T_{12}T_{13}G_{14}G_{15}$-3′-3′-$G_{16}$
G-TBA-C	G_0-5′-5′-$G_1G_2T_3T_4G_5G_6T_7G_8T_9G_{10}G_{11}T_{12}T_{13}G_{14}G_{15}$-3′-3′-$C_{16}$
TBA-A nat	5′-$G_1G_2T_3T_4G_5G_6T_7G_8T_9G_{10}G_{11}T_{12}T_{13}G_{14}G_{15}A_{16}$-3′
TBA-T nat	5′-$G_1G_2T_3T_4G_5G_6T_7G_8T_9G_{10}G_{11}T_{12}T_{13}G_{14}G_{15}T_{16}$-3′

In particular, we have focused our attention to TBA-A (Fig. 1) which, among the derivatives characterized by higher affinities to the target than the TBA, has shown the highest increase in the melting temperature (ΔT_m = +11 °C), in an effort to understand the origin of this extra stability in view of extending this simple modification to other biologically promising G-quadruplex aptamers.

Furthermore, the structures of TBA-A and TBA-T have been compared, in order to highlight the differences in their behaviors.

Results and discussion

NMR spectroscopy and molecular modelling

The one-dimensional ^{1}H NMR spectra (700 MHz, T = 25 °C) of all the modified thrombin aptamers under the PBS buffer conditions used here (see the Experimental section for details) show the presence of no less than eight well-defined signals in the region of 11.5–12.3 ppm, attributable to the imino protons involved in the Hoogsteen hydrogen bonds of at least two G-tetrads. Moreover, more than fifteen main signals in the aromatic region, due to the presence of the base protons of the extra residues, in addition to the nine guanine H8 and six thymine H6 protons, as in the case of the parent TBA, are evident. Concerning TBA-A, TBA-T, A-TBA-T, TBA-G and TBA-C, the simple appearance of their 1D spectra indicates that these modified oligomers form a main single well-defined hydrogen-bonded conformation (Fig. 2). In some cases, weak resonances are observable in the aromatic region of few samples, probably attributable to the unfolded species, considering that their relative intensities turned out to be sensitive to temperature changes (data not shown). On the other hand, in the cases of T-TBA-A, G-TBA-C and C-TBA-G, the imino resonances are spread over a broader spectral region (10.5–12.8 ppm), which appear larger and, importantly, their signals are more than the expected eight for two G-tetrads (Fig. S1 in the ESI†).

Taking into account the good quality of the ^{1}H NMR spectra of TBA-A, TBA-T, A-TBA-T, TBA-G and TBA-C, together with the data concerning the thermal stability experiments and the thrombin affinity test,[16] we have focused our attention

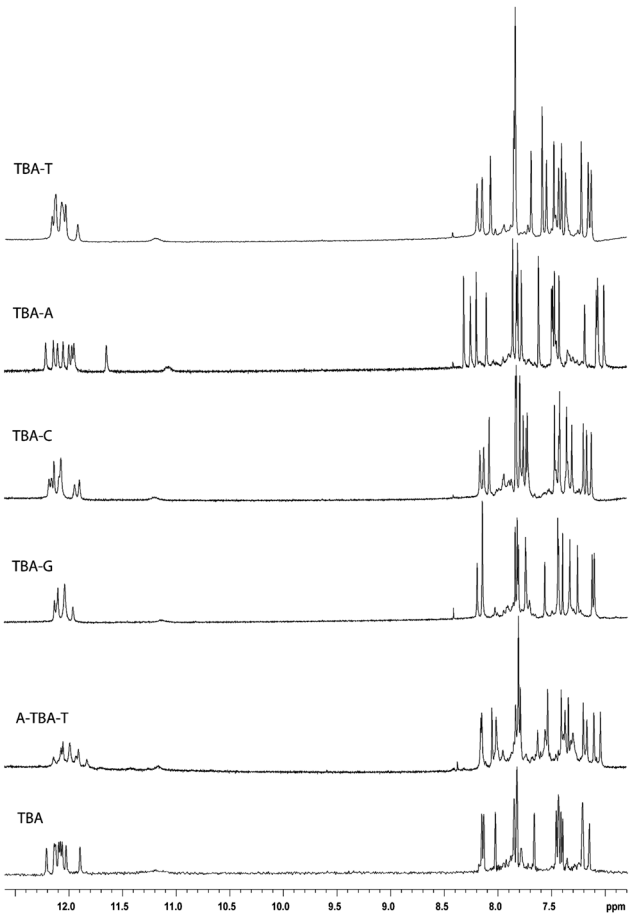

Fig. 2 Aromatic and imino proton regions of the ^{1}H NMR spectra (700 MHz, T = 25 °C) of the TBA analogues and their natural counterpart in PBS buffer solution (H_2O/D_2O 9 : 1) and 0.2 mM EDTA (pH 7.0).

on these five TBA analogues, thus performing further NMR investigations. A combination of the analysis of the 2D NOESY (Fig. 3 and S2 in ESI†) and TOCSY spectra (data not shown) has allowed us to obtain almost complete assignments of the non-exchangeable protons (Table S1 in the ESI†).

All the five TBA analogues investigated in detail share the below described NMR features. The intensities of NOESY crosspeaks between the aromatic base proton and sugar H1′ resonances indicate that four Gs (G_1, G_5, G_{10} and G_{14}) adopt *syn* glycosidic conformations while five Gs (G_2, G_6, G_8, G_{11} and G_{15}) adopt *anti* conformations, where the H8 resonances of the *syn* G residues are upfield shifted with respect to those of the *anti* G residues.[17] On the other hand, all of the thymidines and the extra-residues show *anti* glycosidic conformations. The crosspeak patterns show that four *anti*-Gs (G_2, G_6, G_{11} and G_{15}) have classical H8/H2′–H2″ sequential connectivities to 5′ neighboring *syn*-Gs (G_1, G_5, G_{10} and G_{14}, respectively), thus indicating that the subunits 5′-G_1G_2-3′, 5′-G_5G_6-3′, 5′-$G_{10}G_{11}$-3′ and 5′-$G_{14}G_{15}$-3′ are involved in the formation of a four-stranded helical structure. In summary, as observed for the unmodified TBA, there are 5′-G*syn*G*anti*-3′ steps along each strand connecting the two tetrads.[3] Moreover, the entire pattern of NOEs observed for all the cited Gs indicates that the backbone conformation of these tracts resembles those of the canonical TBA, possessing a right-handed helix structure. The alternation of *syn* and *anti* G residues within each strand suggests that, as in the case of the natural TBA, all the modified oligomers fold into a monomolecular chair-like foldback G-quadruplex structure, characterized by two G tetrads.

Since interresidue NOEs are typically weak for 5′-*anti-syn*-3′ steps,[18] there are two strings of 5′-GGTT-3′ connectivities, namely 5′-$\underline{G}_1G_2T_3T_4$-3′ and 5′-$\underline{G}_{10}G_{11}T_{12}T_{13}$-3′ (where *syn* G residues are underlined). Further additional connectivities are present for the segments 5′-$\underline{G}_5G_6T_7G_8T_9$-3′ and 5′-$\underline{G}_{14}G_{15}$-3′ and the corresponding stretches, identified on the basis of *anti–anti* connectivities. There are no sequential connectivities between the 3′-side thymidines in each loop (T_4, T_9, and T_{13}) and the following *syn*-G.

These two- to four-residue stretches of sequential connectivities were arranged taking into account the primary sequence and the information in long-range NOE connectivities.

As in the case of the parent TBA, for all the modified TBAs studied, there are a number of NOE connectivities observed between the residues not adjacent in the sequence. In particular, NOEs are present between H8 of G_2 and methyl, H2′ and H2″ of T_4 and between H8 of G_{11} and methyl, H2′ and H2″ of T_{13}. Complementary information is provided by the NOEs from the methyl of T_4 with H1′, H2′ and H2″ of G_2 and from the methyl of T_{13} with H1′, H2′ and H2″ of G_{11}. This collection of NOEs places T_4 and T_{13} residues close to the G_2–G_5–G_{11}–G_{14} tetrad. There are NOE connectivities also between H8 of G_8 and H1′, H2′ and H2″ of G_6 and between H1′ of T_9 and H8 of G_{15}, thus indicating that G_8 and T_9 residues in the TGT loop are near to the G_1–G_6–G_{10}–G_{15} tetrad. This collection of NOEs showed that, as strongly suggested by the CD data,[16] all the modified TBAs investigated by NMR adopt G-quadruplex structures strictly resembling that of their natural counterpart.

Remarkably, modified TBAs are characterized by additional NOEs between the extra-residues at the inversion of polarity sites and the deoxyguanosines of the upper tetrad. In particular, NOE connectivities have been observed between H1′/G_{15} and H2′ and H2″/A_{16}, H2″/G_{10} and H8/A_{16}, for TBA-A (Fig. 3); H2″/G_{15} and H8/G_{16} for TBA-G; H8/G_1 and CH_3/T_{16}, H8/G_{15} and H1′/T_{16} for TBA-T; H6/C_{16} and H1′/G_{15} for TBA-C; H8/G_1 and CH_3/T_{16}, H8/G_1 and H2′ and H2″/A_0, H6/T_{16} and H2′ and H2″/A_0 in the case of A-TBA-T (Fig. S2 in the ESI†). This collection of NOE contacts suggests that the extra-residues in the above cited samples are not randomly oriented, but are positioned on the top of the G4 core. In order to corroborate the validity of these considerations the molecular models of TBA-A and TBA-T were built (Fig. 4 and 5), these TBA analogues being among the most stable in the series. As expected, the insertion of an extra adenosine or thymidine residue with a 3′–3′ inversion of the polarity site does not significantly affect the general folding of the modified G-quadruplex structures, compared to the original TBA, as already suggested by the NMR data. It is however noteworthy that, in the case of TBA-A, a close examination of the regions comprising the upper tetrad

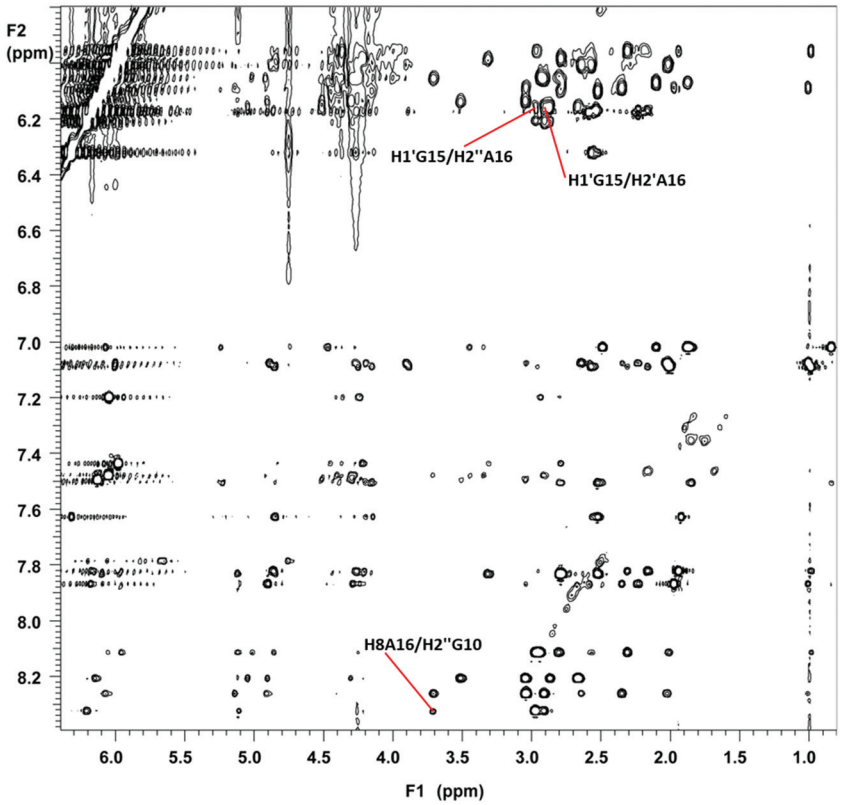

Fig. 3 Expanded region of the 2D NOESY spectrum of TBA-A (700 MHz; 25 °C; strand concentration of 2 mM in PBS buffer solution (H_2O/D_2O 9 : 1) and 0.2 mM EDTA (pH 7.0); total volume 0.6 ml; mixing time 180 ms) correlating bases H8/H6 and anomeric with sugar protons. The NOEs involving the extra-residue are highlighted.

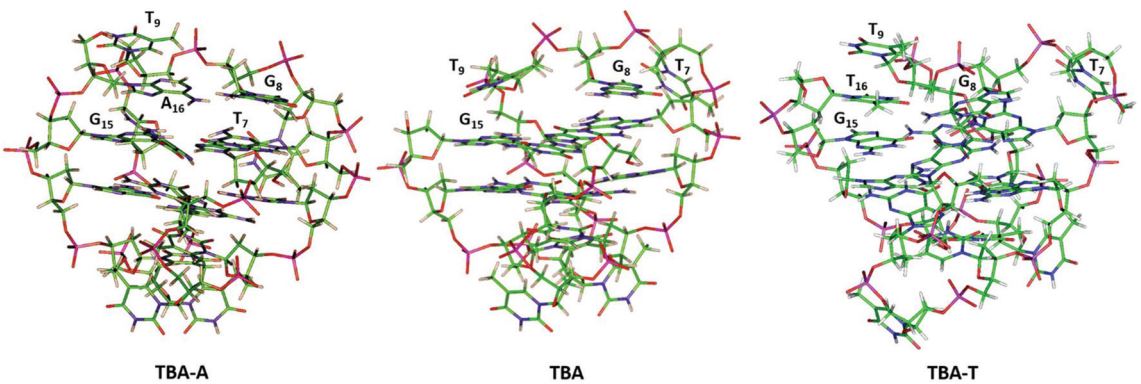

Fig. 4 Stick models of TBA-A, the original TBA and TBA-T. The atoms are shown with different colors (carbons, green; nitrogens, blue; oxygens, red; hydrogens, white; phosphorus, purple).

with the extra 3′–3′ adenosine (A_{16}) and the TGT loop reveals a peculiar kind of intercalation in which A_{16} is sandwiched between the residues T_9 and G_{15}, thus allowing a very efficient stacking interaction among them (Fig. 5). This particular arrangement makes possible the occurrence of H-bonds between the N1 of A_{16} and the $(NH_2)2$ of G_8 and, moreover, between the 5′-OH of A_{16} and the O4 of T_9. Furthermore, another significant difference between TBA-A and TBA regarding the T_7 residue position is that, in the modified aptamer it is placed in close proximity of its upper G-tetrad, while in the parent TBA lies away from the core of the G-quadruplex structure, thus resulting in being exposed to the solvent (Fig. 4). As far as the model of TBA-T is concerned, the extra residue T_{16} shows a similar behavior to A_{16} in TBA-A, being intercalated between the residues T_9 and G_{15}. However, in this case, no H-bonds involving the extra residue have been observed and residue T_9 is less efficiently stacked on the extra residue T_{16}. These differences could account for the higher melting

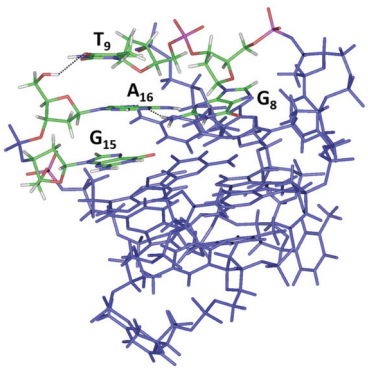

Fig. 5 Lateral view of the TBA-A stick model highlighting the stacking interactions among residues G_{15}, A_{16} and T_9. The atoms of the labelled residues are shown with different colors (carbons, green; nitrogens, blue; oxygens, red; hydrogens, white; phosphorus, purple). Black dotted lines indicate hydrogen bonds involving the extra residue A_{16}.

temperature observed for TBA-A. Moreover, differently from TBA-A, the residue of T_7 in TBA-T arranges outward, similarly to the parent TBA.

CD thermal denaturation measurements

The thermal stability of the TBA analogues was determined by CD melting experiments. The thermodynamic parameters and the melting temperatures obtained by the van't Hoff analysis of the CD melting curves[16] in PBS are shown in Table 2. Inspection of Table 2 reveals that all the TBA analogues have higher melting temperatures compared with the TBA, with the exception of A-TBA-T showing a T_m similar to the TBA. A detailed thermodynamic analysis shows that the addition of an extra nucleotide with inversion of polarity leads to higher $\Delta H_{v.H.}$ and $\Delta S_{v.H.}$, thus suggesting that TBA-A, TBA-G, TBA-C and TBA-T form a more structured folded state stabilised by the presence of additional interactions in comparison with the unmodified TBA. This conclusion is fully consistent with the NMR and modelling results obtained for TBA-A.

Furthermore, we found higher $\Delta H_{v.H.}$ values for TBA-G and TBA-A ($\Delta\Delta H_{v.H.} \sim +48$ kJ mol^{-1}) with respect to TBA-T and TBA-C ($\Delta\Delta H_{v.H.} \sim +25$ kJ mol^{-1}). This observation reveals that purines are able to establish stronger interactions with respect to the pyrimidines. Interestingly, the comparison of the $\Delta H_{v.H.}$ values obtained for TBA-A and TBA-T with the ones for T-TBA-A and A-TBA-T, respectively, reveals that the addition of an extra 5′–5′ nucleotide decreases the enthalpy contribution to the quadruplex stability. On the other hand, the addition of an extra nucleotide through a natural 3′–5′ phosphodiester bond (TBA-A nat and TBA-T nat), does not change the thermodynamic parameters of the TBA (within the experimental error), thus confirming that the presence of the 3′–3′ polarity inversion site is a crucial structural feature in determining the higher thermodynamic stability of the TBA analogues. It should be noted that other authors have reported the synthesis and investigations of TBA derivatives carrying an acridine moiety, a quindoline moiety or both at the 3′-end.[19] Also in these cases, increases of the melting temperatures were observed. However, no NMR and molecular modelling data were reported suggesting a type of intercalation similar to that we observed for TBA-A and TBA-T.

Since stability and folding of G-quadruplex structures strongly depend on the nature of cations in solution, we have also recorded CD spectra and CD melting and annealing curves in potassium buffer of the modified aptamers TBA-A, TBA-T, TBA-C and TBA-G that are among the TBA derivatives characterized by a major structure, which have shown thermal stabilities in PBS higher than the natural TBA (Fig. S3, S4 and Table S2 in ESI†). The CD profiles of the four TBA analogues are quite similar to the natural TBA, thus suggesting that they adopt antiparallel "chair-like" G-quadruplex structures also under these conditions. Concerning the melting experiments, the four ODNs considered confirm their higher stabilities compared with the TBA, although the differences have been proven to be lesser. As for PBS buffer, TBA-A has resulted to be the most stable, while TBA-T has shown a higher T_m than TBA-C and TBA-G. Furthermore, the melting and annealing profiles have resulted to be almost superimposable, thus indicating the occurrence of a monomolecular G-quadruplex structure, as in the case of the natural TBA.

Table 2 Thermodynamic parameters of some modified aptamers and their natural counterpart (TBA) in PBS buffer obtained from the van't Hoff analysis of the CD melting curves (see the text for details)

Names	T_m (°C) (±1)	ΔT_m	$\Delta H_{v.H.}$[a] (kJ mol^{-1})	$\Delta S_{v.H.}$[a] (kJ mol^{-1} K^{-1})
TBA	33	—	124	0.40
TBA-A	44	+11	170	0.54
TBA-T	39	+6	150	0.48
A-TBA-T	33	0	140	0.46
T-TBA-A	36	+3	145	0.47
TBA-G	39	+6	175	0.56
TBA-C	38	+5	148	0.48
TBA-A nat	33	0	130	0.42
TBA-T nat	33	0	130	0.42

[a] The errors on $\Delta H_{v.H.}$ and $\Delta S_{v.H.}$ are within the 10%.

Gel electrophoresis

With an aim to confirm that all the TBA analogues containing the sites of inversion of polarity can adopt the monomolecular G-quadruplex structure characteristic of the natural TBA, a non-denaturing PAGE analysis was performed (Fig. S5 in the ESI†). Except for G-TBA-C, the electrophoretic profile shows that all TBA analogues form main structures with motilities very similar to that of the natural TBA. Taking into account that the electrophoretic motility of G-quadruplex structures is mostly affected by their conformation and that the charge/residue ratio is very similar for all oligonucleotides, the PAGE results strongly suggest the occurring of G-quadruplex conformations comparable to that of the original TBA. However, in the cases of some TBA analogues containing two sites of inversion of polarity (namely, A-TBA-T, T-TBA-A and C-TBA-G) a migration slightly slower than the TBA analogues with one

inversion site was observed, probably due to the hindrance of the two extra residues to move through the gel. In the case of G-TBA-C, the presence of more than one band would suggest the presence of more conformations.

Conclusions

Among the aptamers adopting a G-quadruplex structure, the TBA is probably the most studied and it is still the subject of several investigations. Most of the post-SELEX modifications proposed for this aptamer, with an aim to improve its biological and physical–chemical properties, have concerned the replacement of natural residues with modified ones. Depending on the type of the modified residue used and its position in the sequence, unpredictable results have been obtained, particularly if the modification involves TT loop residues. In a recent communication, we showed that noteworthily improved TBA properties could be obtained simply by linking a natural extra-residue at the 3′-end or at both the ends of the sequence through 3′–3′ or 5′–5′ phosphodiester bonds, and then to protect the conformation of the TT loops from being affected, which is mostly responsible for the interaction with the target. The NMR analysis on TBA-A, TBA-G, TBA-T, TBA-C and A-TBA-T shows that these modified aptamers adopt chair-like G-quadruplex conformations very similar to that of their natural counterpart. Furthermore, NOE contacts involving the extra-residues and one or more guanosines of the upper G-tetrad suggest that extra-residues are not randomly oriented, but stacked on the top of the G-quadruplex structure. The analysis of the thermodynamic parameters shows that all the TBA analogues containing only a 3′–3′ extra-residue are characterized by melting temperatures higher than the TBA (ΔT_m ranging from +5 to +11). Most importantly, the comparison of the thermodynamic data concerning TBA-A nat and TBA-T nat, on one hand, and TBA-A and TBA-T, on the other hand, clearly shows that the presence of only a 3′ extra-residue in the sequence does not result in higher melting temperatures and, then, the occurrence of the 3′–3′ phosphodiester bond is fundamental for improving the thermal stabilities of the modified aptamers. Taking into account the couples TBA-A and T-TBA-A, TBA-T and A-TBA-T, and TBA-G and C-TBA-G,[16] the thermodynamic data suggest also that the presence of the 5′–5′ bonded extra-residue counters the stabilizing effect of the 3′–3′ bonded extra-residue in three cases out four. The remarkable increase obtained in thermal stability, and in the general properties of the TBA, by adding a 3′–3′ extra-residue suggests that this modification could be successfully applied also in improving the properties of other G-quadruplex forming aptamers.

Experimental section

Oligonucleotide synthesis and purification

ODNs containing inversion of polarity sites were synthesized and purified as reported before.[16] ODNs TBA-A nat and TBA-T nat were synthesized using a Millipore Cyclone Plus DNA synthesizer using solid phase β-cyanoethyl phosphoramidite chemistry at the 15 μmol scale. The oligomers were detached from the support and deprotected by treatment with concentrated aqueous ammonia at 80 °C overnight. The combined filtrates and washings were concentrated under reduced pressure, redissolved in H_2O, analyzed and purified by high-performance liquid chromatography on a Nucleogel SAX column (Macherey-Nagel, 1000-8/46), using buffer A: 20 mM NaH_2PO_4/Na_2HPO_4 aqueous solution (pH 7.0) containing 20% (v/v) CH_3CN and buffer B: 1 M NaCl, 20 mM NaH_2PO_4/Na_2HPO_4 aqueous solution (pH 7.0) containing 20% (v/v) CH_3CN; a linear gradient from 0 to 100% B for 45 min and flow rate 1 ml min^{-1} were used. The fractions of the oligomers were collected and successively desalted by Sep-pak cartridges (C-18). The isolated oligomers proved to be >98% pure by HPLC (Fig. S6 in the ESI†).

NMR spectroscopy and molecular modelling

NMR samples were prepared at a concentration of about 2 mM, in 0.6 ml (H_2O/D_2O 9 : 1 v/v) of a PBS buffer solution (pH 7.0) and 0.2 mM EDTA. All the samples were heated for 5–10 min at 80 °C and slowly cooled (10–12 h) to room temperature. The solutions were equilibrated for 24 hours at 4 °C. The annealing process was assumed to be complete when the ^{1}H NMR spectra were super-imposable on changing time. The NMR spectra were recorded with a Varian Unity INOVA 700 MHz spectrometer. The 1D proton spectra of the sample in H_2O were recorded using pulsed-field gradient DPFGSE for H_2O suppression.[20] ^{1}H chemical shifts were referenced relative to external sodium 2,2-dimethyl-2-silapentane-5-sulfonate (DSS). The pulsed-field gradient DPFGSE sequence was used for NOESY[21] (250 ms and 180 ms mixing times) and TOCSY[22](120 ms mixing time) experiments in H_2O. All experiments were conducted using the STATES-TPPI procedure for quadrature detection.[23] In all 2D experiments, the time domain data consisted of 2048 complex points in t2 and 400–512 fids in t1 dimension. A relaxation delay of 1.2 s was used for all experiments.

The main conformational features of the quadruplex adopted by TBA-A and TBA-T were explored by means of a molecular modelling study. The CVFF force field using a CVFF atom types set was used.[24] The initial coordinates for the starting model of TBA-A and TBA-T were taken from the NMR solution structure of the G-quadruplex d(GGTTGGTGTGGTTGG) (Protein Data Bank entry number 148D), with the first and the best representative conformer of the twelve available ones submitted by Feigon *et al.*[25] The initial $5'G_1G_2T_3T_4G_5G_6T_7G_8T_9G_{10}G_{11}T_{12}T_{13}G_{14}G_{15}3'$-$3'A_{16}$ (TBA-A) and $5'G_1G_2T_3T_4G_5G_6T_7G_8T_9G_{10}G_{11}T_{12}T_{13}G_{14}G_{15}3'$-$3'T_{16}$ (TBA-T) G-quadruplex models were built by adding an extra adenosine or thymidine residue, respectively, at the 3′-end of the TBA sequence, linked through a 3′–3′ phosphodiester bond, using the Biopolymer building tool of Discover. The calculations were performed using a distance-dependent macroscopic dielectric constant of 4*r* and an infinite cut-off for non-bonded interactions to partially compensate for the lack of the solvent used.[26] Using steepest descent and conjugate

gradient methods, the conformational energy of the complexes was minimized until convergence to an RMS gradient of 0.1 kcal mol^{-1} $Å^{-1}$ was reached. The illustrations of the structure were generated using the INSIGHT II program, version 2005 (Accelrys, San Diego, CA, USA). All the calculations were performed on a PC running Linux ES 2.6.9.

CD thermal denaturation measurements

The CD samples of modified oligonucleotides and their natural counterpart were prepared at an ODN concentration of 100 μM using a PBS buffer or a potassium buffer (10 mM KH_2PO_4/K_2HPO_4, 70 mM KCl, pH 7.0) and subjected to the annealing procedure (heating at 90 °C and slowly cooling to room temperature). CD melting curves were registered as a function of temperature from 20 °C to 90 °C for all quadruplexes at their maximum Cotton effect wavelengths. The CD data were recorded using a 0.1 cm pathlength cuvette with a scan rate of 0.5 °C min^{-1}. The CD melting curves were modelled by a two-state transition according to the van't Hoff analysis.[27] The melting temperature (T_m), the enthalpy change ($\Delta H_{v.H.}$) and the entropy change ($\Delta S_{v.H.}$) values (Table 2) provide the best fit of the experimental melting data.

Gel electrophoresis

All oligonucleotides were analyzed by non-denaturing PAGE. Samples in the NMR buffer were loaded on a 20% polyacrylamide gel containing Tris-Borate-EDTA (TBE) 2.5× and NaCl 50 mM. The run buffer was TBE 1× containing 100 mM NaCl. For all samples, a solution of glycerol/TBE 1× with 100 mM NaCl 2 : 1 was added just before loading. Electrophoresis was performed at 8 V cm^{-1} at a temperature close to 10 °C. The bands were visualized by UV shadowing.

References

1 F. Radom, P. M. Jurek, M. P. Mazurek, J. Otlewski and F. Jeleń, *Biotechnol. Adv.*, 2013, **31**, 1260.

2 (*a*) A. Varizhuk, N. Ilyinsky, I. Smirnov and G. Pozmogova, *Mini-Rev. Med. Chem.*, 2016, DOI: 10.2174/1389557516666160321114715; (*b*) W. O. Tucker, K. T. Shum and J. A. Tanner, *Curr. Pharm. Des.*, 2012, **18**, 2014.

3 R. F. Macaya, P. Schultze, F. W. Smith, J. A. Roe and J. Feigon, *Proc. Natl. Acad. Sci. U. S. A.*, 1993, **90**, 3745.

4 V. Đapić, V. Abdomerović, R. Marrington, J. Peberdy, A. Rodger, J. O. Trent and P. J. Bates, *Nucleic Acids Res.*, 2003, **31**, 2097.

5 M. Scuotto, E. Rivieccio, A. Varone, D. Corda, M. Bucci, V. Vellecco, G. Cirino, A. Virgilio, V. Esposito, A. Galeone, N. Borbone, M. Varra and L. Mayol, *Nucleic Acids Res.*, 2015, **43**, 7702.

6 L. Bonifacio, F. Church and M. Jarstfer, *Int. J. Mol. Sci.*, 2008, **9**, 422.

7 (*a*) A. Pasternak, F. J. Hernandez, L. M. Rasmussen, B. Veste and J. Wengel, *Nucleic Acids Res.*, 2011, **39**, 1155; (*b*) T. N. Jensen, J. R. Henriksen, B. E. Rasmussen, L. M. Rasmussen, T. L. Andresen, J. Wengel and A. Pasternak, *Bioorg. Med. Chem.*, 2011, **19**, 4739.

8 (*a*) T. Coppola, M. Varra, G. Oliviero, A. Galeone, G. D'Isa, L. Mayol, E. Morelli, M. R. Bucci, V. Vellecco, G. Cirino and N. Borbone, *Bioorg. Med. Chem.*, 2008, **16**, 8244; (*b*) N. Borbone, M. Bucci, G. Oliviero, E. Morelli, J. Amato, V. D'Atri, S. D'Errico, V. Vellecco, G. Cirino, G. Piccialli, C. Fattorusso, M. Varra, L. Mayol, M. Persico and M. Scuotto, *J. Med. Chem.*, 2012, **55**, 10716; (*c*) M. Scuotto, M. Persico, M. Bucci, V. Vellecco, N. Borbone, E. Morelli, G. Oliviero, E. Novellino, G. Piccialli, G. Cirino, M. Varra, C. Fattorusso and L. Mayol, *Org. Biomol. Chem.*, 2014, **12**, 5235.

9 A. Virgilio, M. Varra, M. Scuotto, A. Capuozzo, C. Irace, L. Mayol, V. Esposito and A. Galeone, *ChemBioChem*, 2014, **15**, 652.

10 B. Cai, X. Yang, L. Sun, X. Fan, L. Li, H. Jin, Y. Wu, Z. Guan, L. Zhang, L. Zhang and Z. Yang, *Org. Biomol. Chem.*, 2014, **12**, 8866.

11 A. Virgilio, L. Petraccone, M. Scuotto, V. Vellecco, M. Bucci, L. Mayol, M. Varra, V. Esposito and A. Galeone, *ChemBioChem*, 2014, **15**, 2427.

12 A. Virgilio, L. Petraccone, V. Vellecco, M. Bucci, M. Varra, C. Irace, R. Santamaria, A. Pepe, L. Mayol, V. Esposito and A. Galeone, *Nucleic Acids Res.*, 2015, **43**, 10602.

13 C. G. Peng and M. J. Damha, *Nucleic Acids Res.*, 2007, **35**, 4977.

14 M. Zaitseva, D. Kaluzhny, A. Shchyolkina, O. Borisova, I. Smirnov and G. Pozmogova, *Biophys. Chem.*, 2010, **146**, 1.

15 A. M. Varizhuk, V. B. Tsvetkov, O. N. Tatarinova, D. N. Kaluzhny, V. L. Florentiev, E. N. Timofeev, A. K. Shchyolkina, O. F. Borisova, I. P. Smirnov, S. L. Grokhovsky, A. V. Aseychev and G. E. Pozmogova, *Eur. J. Med. Chem.*, 2013, **67**, 90.

16 V. Esposito, M. Scuotto, A. Capuozzo, R. Santamaria, M. Varra, L. Mayol, A. Virgilio and A. Galeone, *Org. Biomol. Chem.*, 2014, **12**, 8840.

17 (*a*) K. Y. Wang, S. McCurdy, R. G. Shea, S. Swaminathan and P. H. Bolton, *Biochemistry*, 1993, **32**, 1899; (*b*) F. W. Smith and J. Feigon, *Biochemistry*, 1993, **32**, 8682; (*c*) Y. Wang and D. J. Patel, *Structure*, 1993, **1**, 263.

18 (*a*) F. J. M. Van de Ven and C. W. Hilbers, *Eur. J. Biochem.*, 1988, **178**, 1; (*b*) G. M. Clore and A. M. Gronenborn, *CRC Crit. Rev. Biochem. Mol. Biol.*, 1989, **24**, 479; (*c*) K. Wüthrich, *NMR of Proteins and Nucleic Acids*, Wiley, New York, 1986.

19 A. Aviñó, S. Mazzini, R. Ferreira and R. Eritja, *Bioorg. Med. Chem.*, 2010, **18**, 7348.

20 C. Dalvit, *J. Biomol. NMR*, 1998, **11**, 437.

21 J. Jeener, B. Meier, H. P. Bachmann and R. R. Ernst, *J. Chem. Phys.*, 1979, **71**, 4546.

22 L. Braunschweiler and R. R. Ernst, *J. Magn. Reson.*, 1983, **53**, 521.

23 D. Marion, M. Ikura, R. Tschudin and A. Bax, *J. Magn. Reson.*, 1989, **85**, 393.

24 (*a*) J. R. Maple, M.-J. Hwang, T. P. Stockfisch, U. Dinur, M. Waldman, C. S. Ewing and A. T. Hagler, *J. Comput.*

Chem., 1994, **15**, 162; (*b*) W. R. Rudnicki and B. Lesyng, *Comput. Chem.*, 1995, **19**, 253.
25 P. Schultze, R. F. Macaya and J. Feigon, *J. Mol. Biol.*, 1994, **235**, 1532.
26 S. J. Weiner, P. A. Kollman, D. A. Case, U. C. Singh, C. Ghio, G. Alagona, S. Profeta and P. J. Weiner, *J. Am. Chem. Soc.*, 1984, **106**, 765.
27 L. A. Marky and K. J. Breslauer, *Biopolymers*, 1987, **26**, 1601.